

# Electronic zero-point fluctuation forces inside circuit components

Ephraim Shahmoon<sup>1</sup> and Ulf Leonhardt<sup>2</sup>

<sup>1</sup>*Department of Physics, Harvard University, Cambridge MA 02138, USA*

<sup>2</sup>*Department of Physics of Complex Systems, Weizmann Institute of Science, Rehovot 761001, Israel*  
(Dated: December 13, 2016)

One of the most intriguing manifestations of quantum zero-point fluctuations are the van der Waals and Casimir forces, often associated with vacuum fluctuations of the electromagnetic field. Here we study generalized fluctuation potentials acting on internal degrees of freedom of components in electrical circuits. These electronic Casimir-like potentials are induced by the zero-point current fluctuations of any general conductive circuit. For realistic examples of an electromechanical capacitor and a superconducting qubit, our results reveal the possibility of tunable repulsive and attractive forces between the capacitor plates, or the level shifts of the qubit, respectively. Our analysis suggests an alternative route towards the exploration of Casimir-like fluctuation potentials, namely, by characterizing and measuring them as a function of parameters of the environment. Such tunable potentials may be useful for future nano-electromechanical technologies.

Understanding the role of quantum phenomena in electrical circuits has opened numerous possibilities in quantum information and optics [1, 2]. In this Letter we show how conceptually simple systems, such as linear electrical circuits, provide a new direction in the study and application of quantum fluctuation phenomena, in analogy to the van der Waals (vdW) and Casimir forces [3–5]. A key element of the ensuing discussion is the generalization of the familiar Casimir force in three aspects; namely, the source of the quantum fluctuations, the physical effect they entail and, most importantly, how the effect is measured and manipulated.

The Casimir and vdW forces are typically associated with quantum zero-point fluctuations of the electromagnetic field modes. A physical system coupled to these modes then acquires additional potential energy, which for a composite system, leads to a force between its components, e.g. a pair of particles or surfaces in the case of vdW or Casimir, respectively. Nevertheless, such a quantum-fluctuation-driven potential may exist for any system that can exchange energy with a quantum reservoir, following the fluctuation-dissipation theorem [6–9]. In the case of electrical circuits considered here, we employ this principle within the framework of circuit theory, by considering the quantum, zero-temperature noise emerging from resistive circuit elements, in analogy to the Johnson-Nyquist noise at finite-temperatures [10].

After identifying the source of quantum fluctuations in the circuit, we turn to study how its associated energy potentials affect non-resistive components within the circuit. Referring back to effects induced by the electromagnetic vacuum, these include energy level shifts in atoms (Lamb shift) [7, 11], forces between polarizable objects [4, 5, 12–19] and “generalized forces” such as torques [20–23] and lateral forces [24–27]. Equivalently, here we discuss energy shifts in superconducting qubits, or forces/torques acting on internal mechanical degrees of freedom of capacitive elements, all of which driven by the electronic zero-point noise of the circuit (Fig. 1). For

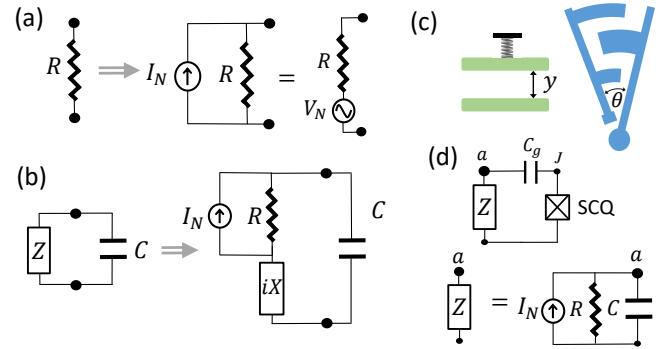


FIG. 1: Generalized potentials induced by electronic quantum fluctuations. (a) Quantum noise source: resistive circuit elements are modeled by a resistor  $R$  in parallel with a current noise source  $I_N$  with the spectrum of Eq. (1) (or equivalently, in series with a voltage  $V_N = RI_N$ ). (b) Capacitor embedded in a general passive circuit represented by its impedance  $Z = R + iX$ . The zero-point-induced potential built on the capacitor, Eq. (3), gives rise to a generalized force  $f = -\partial U / \partial \xi$  on its internal degree of freedom  $\xi$ . (c) Examples of electromechanical capacitors: for the parallel-plate capacitor with separation  $\xi = y$  [28, 29],  $f$  is a force normal to the plates, whereas for the variable capacitor with rotation angle  $\xi = \theta$  [30],  $f$  is a torque. (d) Superconducting qubit (SCQ) capacitively coupled to a circuit  $Z$  (bottom: specific example of an  $RC$  circuit). The zero-point fluctuations from  $Z$  induce shifts in the energy levels of the SCQ in analogy to the Lamb shift [Eq. (5)].

the recently realized electromechanical plate capacitor of Ref. [28, 29], we find tunable repulsive and attractive forces between its plates (on top of the familiar Casimir force), which are estimated to be measurable using current technology. All calculations are performed using simple circuit theory combined with a proper renormalization scheme.

An important opportunity opened by the exploration of zero-point fluctuation phenomena in circuits is the pos-

sibility to measure them as a function of various circuit parameters. Casimir-like forces are typically characterized and measured as a function of distance between the interacting objects [18], whereas their surrounding electromagnetic environment remains unchanged between measurements. In contrast, here both the surrounding environment and zero-point fluctuations sources, that are realized by the reactive and resistive components of the circuit, respectively, can be varied between different measurements. Then, the potential (e.g. force) acting on an internal coordinate of a component embedded in the circuit, can be measured as a function of the parameters of the environment while keeping the internal degrees of the component, e.g. the separation between capacitor plates, fixed. This new possibility may have several advantages as discussed below.

*Source of quantum fluctuations.*— The electric conductors that comprise electronic circuits absorb the energy of electromagnetic fields. Hence, following the fluctuation-dissipation theorem, their electronic degrees of freedom must fluctuate. Within circuit theory, this can be accounted for by accompanying any resistance  $R$  in the circuit by a shunt fluctuating current source,  $I_N(t)$ , with a zero mean and a spectrum [9, 31, 32] (Fig. 1a)

$$S_{I_N}(\omega) = \int_{-\infty}^{\infty} dt e^{i\omega t} \langle I_N(t) I_N(0) \rangle = \frac{2\hbar\omega}{R(\omega)} \frac{1}{1 - e^{-\hbar\omega/T}}, \quad (1)$$

$T$  being the temperature.

*Generalized forces inside capacitors.*— We begin with a general analysis of forces inside a capacitor. The time-averaged electromagnetic energy stored inside a capacitor  $C$  is given by

$$U = \frac{1}{2} C \int_{-\infty}^{\infty} \frac{d\omega}{2\pi} S_V(\omega), \quad S_V(\omega) = \frac{1}{T_e} \langle V(\omega) V(-\omega) \rangle, \quad (2)$$

where  $V(\omega) = \int_{-\infty}^{\infty} dt e^{i\omega t} V(t)$  is the Fourier transform of the voltage  $V(t)$  across the capacitor,  $S_V(\omega)$  is its fluctuation spectrum and  $T_e \rightarrow \int_{-\infty}^{\infty} dt = 2\pi\delta(\omega = 0)$  is the duration of the experiment. Therefore, the potential energy  $U$  is determined by the spectrum of the voltage  $V(\omega)$ , that depends on the circuit in which the capacitor is embedded. In the absence of any external sources, a general linear circuit can be characterized by its impedance  $Z(\omega) = R(\omega) + iX(\omega)$ ,  $R$  being its resistive part and  $X$  its reactive part (both real), see Fig. 1b. Taking into account the noise due to the resistance  $R$  and solving the Kirchhoff circuit equations in Fig. 1b at frequency  $\omega$ , we find  $V(\omega)$  in terms of  $I_N(\omega)$ , and insert it into Eq. (2). Using Eq. (1) at zero temperature, we thus obtain the zero-point fluctuation-induced potential built on the capacitor,

$$U = \int_{-\infty}^{\infty} \frac{d\omega}{2\pi} \hbar\omega \frac{R(\omega)C}{[1 + X(\omega)C\omega]^2 + [R(\omega)C\omega]^2}. \quad (3)$$

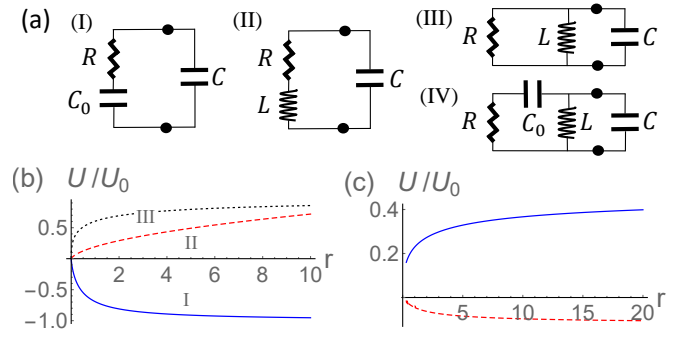


FIG. 2: Potential energy inside a capacitor. (a) Four simple cases for the general circuit of Fig. 1b. (b) Potential energy  $U$ , Eq. (3). For case (I),  $U$  from Eq. (4) is plotted in units of  $U_0 = \hbar/(2\pi RC_0)$  and as a function of  $r = C_0/C$  (solid line). For a parallel-plate capacitor with plate separation  $y \propto r$ , the resulting force between the plates is repulsive. Dashed and dotted lines: same as solid line, for cases (II) and (III) with  $U_0 = \hbar R/L$  and  $U_0 = (\hbar/2\pi)R/L$ , respectively, and  $r = L/(CR^2)$ , both yielding an attractive force for a plate capacitor. (c) Same as (b) for case (IV) with  $U_0 = \hbar/(RC_0)$  and  $r = C_0/C$ . Depending on the parameter  $a = \sqrt{L/C_0}/R$ , both attractive ( $a = 0.5$ , solid line) and repulsive ( $a = 2$ , dashed line) potentials are possible.

For an internal degree of freedom  $\xi$  on which the capacitance  $C(\xi)$  depends, the resulting generalized zero-point force is given by  $f = -\partial U/\partial \xi$ . Examples include a force between the plates of a parallel-plate capacitor with a separation  $\xi = y$ , or a torque in a rotary variable capacitor with an angle  $\xi = \theta$  (Fig. 1c), where the generalization to forces in e.g. variable inductors, is straightforward.

*Some simple circuits.*— Considering first the simplest possible circuit consisting of a resistor  $R$  (frequency independent) coupled to the capacitor  $C$ , we take  $X = 0$  and  $R(\omega) = R$  in Eq. (3), leading to a logarithmic divergence at high frequencies,  $U \sim \int d\omega/\omega$ . Recalling that the lumped-element description used in circuit theory is based on a quasistatic approximation valid for  $\omega \ll c/l$ ,  $l$  being a typical element size, this divergence implies that such long-wavelength description cannot account well for the  $RC$ -circuit situation. This is similar to the divergence encountered by trying to calculate the Lamb shift using the dipole approximation [7], where here the atom and the electromagnetic vacuum are replaced by the capacitor and the resistor, respectively. We note that unlike the case of vdW/Casimir forces, here the divergence in the potential energy also implies a similar divergence in the force along the internal coordinate  $\xi$  [33].

Nevertheless, this divergent potential is useful as a reference energy for the *renormalization* of the potential energy built on the capacitor in other circuits. For example, consider the case (I) in Fig. 2a, where a capacitor  $C_0$  is added in series to the resistor  $R$ . Using  $X = 1/(\omega C_0)$  in

Eq. (3) we again obtain the same logarithmic divergence in  $U$ . Then, upon subtracting the reference result of the  $RC$ -circuit, the integral for the potential converges and we obtain a renormalized finite result [33]

$$U_I = -\frac{\hbar}{2\pi RC_0} r \ln \left( 1 + \frac{1}{r} \right), \quad r = C_0/C. \quad (4)$$

For an internal coordinate  $\xi \propto 1/C \propto r$ , as in a parallel-plate capacitor, this leads to a *repulsive* force, e.g. between capacitor plates, see Fig. 2b. The physical meaning of the above renormalization procedure and its generalization to other circuits are discussed below.

Proceeding to the series  $RLC$  circuit, case (II) in Fig. 2a, we use  $X = -\omega L$  in Eq. (3), and obtain a finite result without the need of renormalization. Here convergence is guaranteed by the existence of the inductor  $L$  in series, whose impedance  $-i\omega L$  disconnects the circuit at high frequencies. For the parallel  $RLC$  of case (III), we find the impedance  $R(\omega) + iX(\omega) = (\omega L + iR) \times \omega LR / [R^2 + (\omega L)^2]$ , and renormalize the integral (3) by subtracting the  $RC$  result. The resulting energy potentials  $U_n = \hbar(R/L)F_n$  for both cases  $n = \text{II, III}$ , are obtained analytically as a function  $F_n(r)$  of the parameter  $r = L/(CR^2)$  [33] and are plotted in Fig. 2b. For  $\xi \propto r$ , the force now becomes attractive in both cases. At the limits  $R \rightarrow 0$  and  $R \rightarrow \infty$  for circuits (II) and (III), respectively, the corresponding asymptotic forms,  $F_{\text{II}}(r \gg 1), F_{\text{III}}(r \ll 1) \approx \sqrt{r}/4$ , both yield the potential,  $U \approx (\hbar/4)/\sqrt{LC}$ , equal to half the zero-point energy of an isolated  $LC$  circuit.

As the last simple example we consider circuit (IV), where the sign of the force can be tuned. At high frequencies, the inductor is effectively disconnected, returning to circuit (I) which exhibited a repulsive force, whereas at very low frequencies  $C_0$  is disconnected, potentially leading to an isolated  $LC$  circuit with an attractive force. Such competing high and low frequency behaviors both contribute to the potential in Eq. (3), which is found as a function of two parameters,  $r = C_0/C$  and  $a = \sqrt{L/C_0}/R$  [33]. For example, Fig. 2c presents the potential as a function of  $r$  for both  $a = 0.5$  (solid line) and  $a = 2$  (dashed line), yielding the possibility of attractive and repulsive forces, respectively, for  $\xi \propto r$ .

*Measurement as a function of circuit parameters.*— As typical of Casimir force measurements, the potential in Figs. 2b,c is effectively plotted as a function of the internal coordinate on which the force acts,  $\xi$ , via its dependence on  $C \propto 1/r$ . However, keeping  $\xi$  (and hence  $C$ ) fixed, we may still vary other parameters of the system wherein the capacitor is embedded, generally represented by its impedance  $Z$ , a possibility that typically does not exist in other Casimir-like setups. In practice this can be achieved by tuning the parameters of circuit components such as variable capacitors, inductors and resistors. While the electronic zero-point force may highly depend on parameters within  $Z$ , this should not be the case for

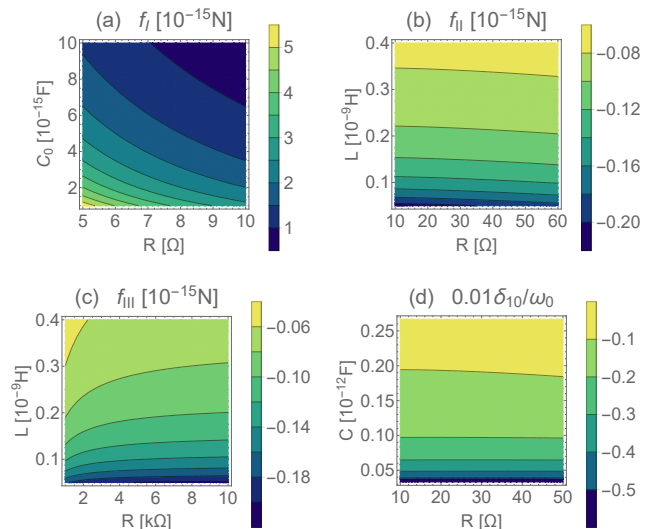


FIG. 3: The ability to measure fluctuation potentials as a function of parameters of the environment (circuit) presents an interesting possibility opened by circuits for fluctuation-induced phenomena. (a,b,c): The force between the capacitor plates in the circuits (I,II,III) from Fig. 2a is plotted as a function of circuit parameters. Circuit (I) exhibits repulsive forces whereas circuits (II) and (III) exhibit attractive forces. In the limits of small  $R$  for  $f_{II}$  and large  $R$  for  $f_{III}$ , both forces become identical to that in the isolated  $LC$  circuit. All three cases are plotted using the physical parameters of the parallel-plate electromechanical capacitor of Ref. [28], whose displacement-measurement sensitivity of  $\sim 10^{-32} \text{m}^2 \text{Hz}^{-1}$  is estimated to be sufficient to detect the sub fN forces we find (text). (d) Shift in the transition frequency of a superconducting transmon qubit with  $\sqrt{E_C/8E_J} = 0.1$ ,  $C_g/C_J = 0.1$  and  $\omega_0 = 2\pi \times 5 \text{GHz}$ . Shifts of the order of 0.1% of the original transition frequency are observed, much larger than the acquired level width (text).

other forces that act on  $\xi$ , such as the familiar Casimir force induced by the electromagnetic vacuum [33]. Therefore, measuring the force on  $\xi$  at a fixed value of  $\xi$ , but as a function of the circuit parameters in  $Z$ , may enable to distinguish the electronic zero-point force from all other forces, which merely contribute a constant offset to the measured force.

The dependence on circuit parameters is illustrated in Fig. 3. For the capacitor  $C$ , we consider the recently realized parallel-plate capacitor with a movable plate, which is cooled to its motional ground state [28, 29]. The plates, of diameter  $15 \mu\text{m}$ , are kept at a fixed separation  $\xi = y = 50 \text{nm}$ . Forces on the movable plate are balanced by a restoring potential, leading to a small displacement in the separation  $y$ , which is measured at high precision [28]. For circuit (I), we plot the repulsive force  $f$  between the plates of  $C$  as a function of the resistor  $R$  and capacitor  $C_0$ , obtaining  $f$  at the fN scale (Fig. 3a). The attractive forces of circuits (II) and (III) are plotted as a

function of the parameters  $R$  and  $L$  (Figs. 3b,c). We estimate that these fN-scale forces are detectable with current technology by using the so-called dynamic method [18]. Namely, around each value of a circuit parameter at which the force is to be measured, a weak modulation of this parameter is introduced. This leads to a measurement of the *derivative* of the force with respect to and as a function of the circuit parameters. Considering the device from Ref. [28], with a displacement sensitivity of  $\sim 10^{-32}\text{m}^2\text{Hz}^{-1}$ , we estimate that sub fN-scale forces are detectable [33].

*Level shifts in a superconducting qubit.*— In addition to forces, the electronic zero-point fluctuations may induce shifts in the quantized energy levels of components such as superconducting qubits (SCQ) embedded in the circuit, in analogy to the Lamb shift in atoms. Such a Lamb shift was measured recently for a SCQ coupled to a microwave cavity or to a magnon [34–36]. Here however, we consider the general dissipative case, where a SCQ is capacitively coupled to a circuit represented by a complex impedance  $Z$  (Fig. 1d). For weak coupling  $C_g \ll C_J$ ,  $C_J$  being the total capacitance of the SCQ, the voltage fluctuations at point  $a$ ,  $V_a(t)$ , are determined by  $Z$  and form an effective reservoir coupled to the charge of the SCQ,  $Q_J$ , via the Hamiltonian  $H_I \approx (C_g/C_J)V_a(t)Q_J$  [31, 37]. Using lowest order perturbation theory, we then find the correction (shift) to the energy difference between the two lowest energy states  $|0\rangle$  and  $|1\rangle$  of a transmon SCQ [33]

$$\delta \approx \frac{\beta^2}{\hbar Z_J} \int_0^\infty \frac{d\omega}{2\pi} S_{V_a}(\omega) \left[ P \frac{\omega_{10}}{\omega_{10}^2 - \omega^2} - \frac{1}{\omega + \omega_{21}} \right], \quad (5)$$

where the corresponding width acquired by the level  $|1\rangle$  is given by  $\gamma \approx \beta^2 S_{V_a}(\omega_{10})/(2\hbar Z_J)$ . Here  $\hbar\omega_{nm}$  is the energy difference between the levels  $n$  and  $m$ ,  $\beta = C_g/C_J$ ,  $Z_J = (\hbar/e^2)\sqrt{E_C/2E_J}$  with  $E_C$  and  $E_J$  the charging and Josephson energies of the SCQ [31, 37], and  $P$  is Cauchy's principal value.

As a specific example, consider a circuit consisting of a resistor  $R$  and capacitor  $C$  in parallel (Fig. 1d). For weak coupling we find  $S_{V_a}(\omega) \approx S_{I_N}(\omega)R^2/(1 + \omega^2 C^2 R^2)$  so that the integral (5) converges, yielding  $\delta \approx -\omega_0(R/Z_J)\beta^2/(2b)$  for  $b \equiv \omega_0 RC \ll 1$ , with  $\omega_0 = \sqrt{8E_C E_J}/\hbar$  [33]. We note that in this regime the shift overwhelms the acquired width,  $|\delta|/\gamma \approx 1/(2b) \gg 1$ . As in the discussion of forces, the shift can be measured as a function of the circuit parameters  $R$  and  $C$ , as illustrated in Fig. 3d, using typical transmon parameters [37]. Shifts of the order of 0.1% of the original qubit resonance,  $\omega_{10} = \omega_0 - E_C/\hbar \approx \omega_0$ , are observed.

*Renormalization procedure.*— Returning to the renormalization scheme used above, we first concentrate on that of circuit (I), which can be understood as follows: The potential energy of the  $RC$ -circuit reflects the energy cost for connecting a resistor  $R$  to a capacitor  $C$ ,

which nevertheless cannot be calculated using circuit theory (it diverges). A reliable result can however be obtained for the extra energy required to introduce additional elements to the system. Therefore  $U_I$  is given by the energy difference between the "bare"  $RC$  and  $RC$  configurations [which indeed vanishes for  $C_0 \rightarrow \infty$  ( $X \rightarrow 0$ )]. This renormalization is similar to that of the vdW energy between a pair of atoms driven by vacuum fluctuations, where the diverging Lamb shift of the individual atoms is subtracted [7, 38]. Likewise, in circuit (I), two capacitors acquire an interaction energy driven by current fluctuations from  $R$ , whereas a finite result is obtained by subtracting the reference "Lamb shift" case of the individual capacitor ( $RC$  circuit energy). We note that in order for the renormalized finite result to comply with circuit theory, the integration over  $\omega$  has to begin converging at frequencies below the cutoff of the theory,  $c/l$  [38]. In case (I) this leads to the validity condition  $1/(RC) \ll c/l$ , whereas similar conditions are found for all other cases [33].

This renormalization procedure can be generalized as follows. For a given circuit, we obtain a "reference circuit" by taking the  $\omega \rightarrow \infty$  limit for the impedances of its components, i.e. short circuit for capacitors and open circuit for inductors. The renormalized energy of the circuit is given by subtracting that of the "reference circuit" from that of the "bare" circuit. Then, by measuring the force/potential as a function of circuit parameters that *do not* appear in the "reference circuit", the reference energy adds only a constant offset to the measured signal. For cases (I), (III) and (IV), the "reference circuit" is the  $RC$  circuit whereas the corresponding references for case (II) and the SCQ are disconnected capacitor and shorted SCQ, respectively, for which the reference energy vanishes. Measurements of the forces  $f_{I,III}$  in Figs. 3a,c are therefore performed at fixed  $R$  and as a function of  $C_0$  and  $L$ , respectively, whereas those of Fig. 3b,d can be performed also as a function of  $R$ .

*Discussion.*— Recent studies of quantum phenomena in electrical circuits have indicated their relevance to Casimir physics [39–41]. Our results suggest that the recent realization of quantum electromechanical systems [28, 29] opens more opportunities for the exploration of fluctuation phenomena. First, a variety of tunable fluctuation forces or level shifts may arise, exhibiting for example repulsive or attractive forces. Second, the new possibility to measure these zero-point electronic potentials as a function of the parameters of the environment, rather than as a function of an interaction distance, may entail several advantages: 1. The ability to distinguish these potentials from other random potentials, such as patch potentials [42–44], means that the limitation on measurement precision imposed by the distance dependence of the latter, now becomes irrelevant. 2. The potentially sensitive dynamic measurement method [18] is natural to apply here, where circuit parameters might be

simple to modulate.

More generally, this work identifies quantum electromechanical circuits as a promising platform for the exploration of Casimir physics beyond the sphere-surface configuration, which is conceptually different from other recent approaches, e.g. using integrated silicon chips [45] or optical tweezers [46]. In this respect, the possibilities allowed for by such systems might go well beyond those found by the above analysis of a few simple circuits, especially considering the generality of our approach and future progress in the recently-realized quantum electromechanical circuits [28]. Moreover, the tunable potentials found above may prove useful for future nanoelectromechanical systems or quantum technologies wherein control of zero-point potentials is essential [47].

We acknowledge fruitful discussions with Itay Griniasty, Konrad Lehnert, Mohammad Hamidian and Homer Reid, and financial support from the MIT-Harvard Center for Ultracold Atoms, ERC and ISF.

- 
- [1] M. H. Devoret and R. J. Schoelkopf, *Science* **339**, 1169 (2013).
  - [2] S. M. Girvin, M. H. Devoret and R. J. Schoelkopf, *Phys. Scr.* **T137**, 014012 (2009).
  - [3] F. London, *Trans. Faraday Soc.* **33**, 8-26 (1937).
  - [4] H. B. G. Casimir and D. Polder, *Phys. Rev.* **73**, 360-372 (1948).
  - [5] H. B. G. Casimir, *Proc. K. Ned. Akad. Wet.* **51**, 793 (1948).
  - [6] I. E. Dzyaloshinskii, E. M. Lifshitz and L. P. Pitaevskii, *Advances in Physics*, **10**, 165 (1961).
  - [7] P. W. Milonni, *The Quantum Vacuum: An Introduction to Quantum Electrodynamics* (Academic, 1993).
  - [8] S. Scheel, in *Forces of the Quantum Vacuum* (W. M. R. Simpson and U. Leonhardt, Eds.), Ch. 3 (World Scientific, 2015).
  - [9] E. Shahmoon, manuscript in preparation.
  - [10] H. Nyquist, *Phys. Rev.* **32**, 110 (1928).
  - [11] M.O. Scully and M. S. Zubairy, *Quantum Optics* (Cambridge University Press, Cambridge, England, 1997).
  - [12] S. K. Lamoreaux, *Phys. Rev. Lett.* **78**, 5 (1997).
  - [13] U. Mohideen and A. Roy, *Phys. Rev. Lett.* **81**, 4549 (1998).
  - [14] H. B. Chan, V. A. Aksyuk, R. N. Kleiman, D. J. Bishop and F. Capasso, *Science* **291**, 1941 (2001).
  - [15] R. S. Decca, D. López, E. Fischbach and D. E. Krause, *Phys. Rev. Lett.* **91**, 050402 (2003).
  - [16] J. Munday, F. Capasso and V. A. Parsegian, *Nature* **457**, 170 (2009).
  - [17] G. Torricelli, P. J. van Zwol, O. Shpak, C. Binns, G. Palasantzas, B. J. Kooi, V. B. Svetovoy and M. Wuttig, *Phys. Rev. A* **82**, 010101(R) (2010).
  - [18] R. S. Decca, in *Forces of the Quantum Vacuum* (W. M. R. Simpson and U. Leonhardt, Eds.), Ch. 5 (World Scientific, 2015).
  - [19] A. W. Rodriguez, F. Capasso and S. G. Johnson, *Nature Photon.* **5**, 211 (2011).
  - [20] V. A. Parsegian and G. H. Weiss, *J. Adhesion* **3**, 259267 (1972).
  - [21] J. N. Munday, D. Iannuzzi, Y. Barash and F. Capasso, *Phys. Rev. A* **71**, 042102 (2005).
  - [22] R. B. Rodrigues, P. A. Maia Neto, A. Lambrecht and S. Reynaud, *Europhys. Lett.* **76**, 822 (2006).
  - [23] R. Esquivel-Sirvent, G. H. Cocoletzi, and M. Palomino-Ovando, *Journal of Applied Physics* **108**, 114101 (2010).
  - [24] T. Emig, A. Hanke, R. Golestanian and Mehran Kardar, *Phys. Rev. Lett.* **87**, 260402 (2001).
  - [25] F. Chen, U. Mohideen, G. L. Klimchitskaya and V. M. Mostepanenko, *Phys. Rev. Lett.* **88**, 101801 (2002).
  - [26] R. B. Rodrigues, P. A. Maia Neto, A. Lambrecht and S. Reynaud, *Phys. Rev. Lett.* **96**, 100402 (2006).
  - [27] K. A. Milton, P. Parashar, J. Wagner and I. Caverio-Pelez, *Journal of Vacuum Science and Technology B* **28**, C4A8 (2010).
  - [28] J. D. Teufel, T. Donner, Dale Li, J. W. Harlow, M. S. Allman, K. Cicak, A. J. Sirois, J. D. Whittaker, K. W. Lehnert and R. W. Simmonds, *Nature* **475**, 359 (2011).
  - [29] R. W. Andrews, A. P. Reed, K. Cicak, J. D. Teufel and K. W. Lehnert, *Nature Commun.* **6**, 10021 (2015).
  - [30] B. Yang, C. Lee, R. K. Kotlanka, J. Xie and S. P. Lim, *J. Micromech. Microeng.* **20**, 065017 (2010).
  - [31] M. H. Devoret, *Quantum Fluctuations in Electrical Circuits*, in *Quantum Fluctuations*, Les Houches Session LXIII, pp. 351 (Elsevier 1997).
  - [32] J. R. Zurita-Sánchez and C. Henkel, *Phys. Rev. A* **73**, 063825 (2006).
  - [33] see Supplemental Material.
  - [34] A. Fragner, M. Göppl, J. M. Fink, M. Baur, R. Bianchetti, P. J. Leek, A. Blais and A. Wallraff, *Science* **322**, 1357 (2008).
  - [35] A. A. Abdumalikov, Jr., O. Astafiev, Y. Nakamura, Y. A. Pashkin and J. Tsai, *Phys. Rev. B* **78**, 180502(R) (2008).
  - [36] Y. Tabuchi, S. Ishino, A. Noguchi, T. Ishikawa, R. Yamazaki, K. Usami and Y. Nakamura, *Science* **349**, 405 (2015).
  - [37] J. Koch, T. M. Yu, J. Gambetta, A. A. Houck, D. I. Schuster, J. Majer, A. Blais, M. H. Devoret, S. M. Girvin, and R. J. Schoelkopf, *Phys. Rev. A* **76**, 042319 (2007).
  - [38] E. Shahmoon, in *Forces of the Quantum Vacuum* (W. M. R. Simpson and U. Leonhardt, Eds.), Ch. 3 (World Scientific, 2015).
  - [39] C. M. Wilson, G. Johansson, A. Pourkabirian, M. Simoen, J. R. Johansson, T. Duty, F. Nori and P. Delsing, *Nature* **479**, 376-379 (2011).
  - [40] P. Lähteenmäki, G. S. Paraoanu, J. Hassel and J. Hakonen, *Proc. Natl. Acad. Sci.* **110**, 4234 (2013).
  - [41] E. Shahmoon, I. Mazets and G. Kurizki, *Proc. Natl. Acad. Sci.* **111**, 10485 (2014).
  - [42] W. M. R. Simpson, U. Leonhardt, R. S. Decca and S. Y. Buhmann, in *Forces of the Quantum Vacuum* (W. M. R. Simpson and U. Leonhardt, Eds.), Ch. 6 (World Scientific, 2015).
  - [43] J. L. Garrett, D. Somers, and J. N. Munday, *J. Phys.: Condens. Matter* **27**, 214012 (2015).
  - [44] R. O. Behunin, F. Intravaia, D. A. R. Dalvit, P. A. Maia Neto and S. Reynaud, *Phys. Rev. A* **85**, 012504 (2012).
  - [45] J. Zou, Z. Marcet, A. W. Rodriguez, M. T. H. Reid, A. P. McCauley, I. I. Kravchenko, T. Lu, Y. Bao, S. G. Johnson and H. B. Chan, *Nat. Commun.* **4**, 1845 (2013).
  - [46] D. S. Ether jr., L. B. Pires, S. Umrath, D. Martinez, Y. Ayala, B. Pontes, G. R. de S. Araújo, S. Frases, G.-L. Ingold, F. S. S. Rosa, N. B. Viana, H. M. Nussenzveig

## Supplemental Materials: Electronic zero-point fluctuation forces inside circuit components

This supplemental document includes two parts. Section 1 is dedicated to the calculation of energy potentials inside a capacitor, and the discussion of some related practical issues. In Sec. 2 we provide the details of the calculation of energy shifts in a transmon superconducting qubit.

### 1. ENERGY POTENTIAL AND FORCE INSIDE A CAPACITOR

#### 1.1 Calculation of the potential for the circuits considered in the main text

We begin with the potential built on the capacitor of the  $RC$  circuit case, obtained by inserting  $R(\omega) = R$  and  $X(\omega) = 0$  in Eq. (3) of the main text,

$$U_{RC} = \int_0^\infty \frac{d\omega}{2\pi} \hbar \omega \frac{RC}{1 + (RC\omega)^2}. \quad (S1)$$

As explained in the main text, this logarithmically divergent result serves as a reference energy for some of the other circuits. For example, in the case of circuit (I) [Fig. 2a in main text], we insert  $R(\omega) = R$  and  $X(\omega) = 1/(\omega C_0)$  into Eq. (3) and obtain the "bare" potential  $\tilde{U}_I$  which diverges as in  $U_{RC}$ . The renormalized potential is then

$$U_I = \tilde{U}_I - U_{RC} = - \int_0^\infty \frac{d\omega}{2\pi} \hbar \omega RC \frac{\frac{C}{C_0} \left(2 + \frac{C}{C_0}\right)}{\left(1 + \frac{C}{C_0}\right)^2 + (RC\omega)^2 \left[1 + \left(1 + \frac{C}{C_0}\right)^2\right] + (RC\omega)^4}. \quad (S2)$$

Upon performing the integral we arrive at Eq. (4) in the main text. The above integral begins converging for  $\omega \gg 1/(RC)$ , where it behaves as  $\int d\omega/\omega^3$ . Since the lumped-element circuit theory we use is essentially a low-frequency theory valid for  $\omega \ll c/l$ , the convergence is meaningful only if it begins for  $\omega$ -values smaller than the cutoff of the theory ( $l$  being a typical size of a circuit element and  $c$  the speed of light) [S1]. This leads to the validity condition,  $1/(RC) \ll c/l$ .

Proceeding to circuit (II) [Fig. 2a in main text], we use  $R(\omega) = R$  and  $X(\omega) = -\omega L$  in Eq. (3), yielding

$$U_{II} = \int_0^\infty \frac{d\omega}{2\pi} \hbar \omega \frac{RC}{(1 - CL\omega^2)^2 + (RC\omega)^2}. \quad (S3)$$

This integral converges as  $\int d\omega/\omega^3$ , a limit which is reached for  $\omega \gg 1/\sqrt{LC}$ ,  $R/L$ , leading to a validity condition  $c/l \gg 1/\sqrt{LC}$ ,  $R/L$ . Changing the integration variable to  $x = CL\omega^2 - 1$ , the integral (S3) can be performed analytically, obtaining

$$U_{II} = \hbar \frac{R}{L} \frac{q}{4} \left[ \sqrt{\frac{1}{-1+4q}} + \frac{2 \arctan\left(\frac{-1+2q}{\sqrt{-1+4q}}\right)}{\pi \sqrt{-1+4q}} \right] \approx \begin{cases} -\hbar \frac{R}{L} \frac{1}{2\pi} q \ln q, & q \ll 1 \\ \hbar \frac{R}{L} \frac{1}{4} \sqrt{q}, & q \gg 1, \end{cases} \quad (S4)$$

with the dimensionless parameter  $q = L/(R^2 C)$ . This analytical result was further verified by comparing it to a direct numerical evaluation of the integral as a function of  $q$ .

For circuit (III), we can either find its impedance in the form  $R(\omega) + iX(\omega)$  (as in main text) or simply solve the Kirchhoff equations for the voltage on the capacitor as a function of  $I_N$ , and use it in Eq. (2) of the main text. In either case, we obtain the "bare" result

$$\tilde{U}_{III} = \int_0^\infty \frac{d\omega}{2\pi} \hbar \omega \frac{\omega^2 L^2 RC}{R^2 (1 - CL\omega^2)^2 + \omega^2 L^2}, \quad (S5)$$



which diverges logarithmically as in (S1). The renormalized result  $U_{\text{III}} = \tilde{U}_{\text{III}} - U_{RC}$  is then given by the integral

$$U_{\text{III}} = \int_0^\infty \frac{d\omega}{2\pi} \hbar \omega RC \frac{(RC\omega)^2 - \left(\frac{R}{L\omega}\right)^2 (1 - \omega^2 LC)^2}{\left[1 + \left(\frac{R}{L\omega}\right)^2 (1 - \omega^2 LC)^2\right] [1 + (RC\omega)^2]}, \quad (\text{S6})$$

whose convergence properties set the validity condition  $c/l \gg 1/\sqrt{LC}, 1/(RC)$ . The integration yields the potential

$$U_{\text{III}} = \hbar \frac{R}{L} \frac{q}{8\pi \sqrt{-1 + \frac{4}{q}}} \left[ \left( \frac{4}{q} - 1 \right) \arctan \left( \frac{-1 + \frac{2}{q}}{\sqrt{-1 + \frac{4}{q}}} \right) + \sqrt{-1 + \frac{4}{q}} \left( \pi \left( -1 + \frac{2}{q} \right) \sqrt{\frac{1}{-1 + \frac{4}{q}}} + 2 \ln q \right) \right], \quad (\text{S7})$$

whose asymptotic forms are given by  $U_{\text{III}}(q \ll 1) \approx \hbar(R/L)\sqrt{q}/4$  and  $U_{\text{III}}(q \gg 1) \approx \hbar(R/L) \left[ \frac{1}{2\pi} + \frac{3-2\ln q}{4\pi q} \right]$ , with the parameter  $q = L/(R^2 C)$  (verified numerically).

Finally, for circuit (IV) we use the same methods described above for circuit (III), and reach the "bare" result

$$\tilde{U}_{\text{IV}} = \int_0^\infty \frac{d\omega}{2\pi} \hbar \omega RC \frac{\omega^4 L^2 C_0^2}{R^2 C_0^2 \omega^2 (1 - \omega^2 LC)^2 + [1 - \omega^2 L(C + C_0)]^2}, \quad (\text{S8})$$

which again diverges as  $U_{RC}$  in (S1). We obtain the renormalized potential in a converging integral form, and as a function of the parameters  $r = C_0/C$  and  $a = \sqrt{L/C_0}/R$ ,

$$U_{\text{IV}} = \frac{\hbar}{RC_0} \frac{r}{4\pi} \int_0^\infty dx \frac{x \{ 2a^2 r(r+1) - r^2 - xa^2 r[2(a^2 - 1)r^2 + a^2 r] \} - 1}{(1+x) \{ r^2 x(1 - a^2 r x)^2 + [1 - xa^2 r(r+1)]^2 \}}. \quad (\text{S9})$$

This integral can be evaluated numerically for different values of  $r$  and  $a$ . Its convergence properties imply the validity condition  $c/l \gg 1/\sqrt{LC}, 1/(RC)$ .

The expressions for the potentials in Eq. (4) of the main text and Eqs. (S4), (S7) and (S9) here, are used for the plots in Fig. 2. In order to calculate the force in Fig. 3, we consider a parallel-plate capacitor with a plate area  $A$  and separation  $y$ ,  $C = A\varepsilon/y$ . Defining the dimensionless potentials  $F$  as

$$U_{\text{I}} = \frac{\hbar}{RC_0} F_{\text{I}}(r), \quad U_{\text{II}} = \hbar \frac{R}{L} F_{\text{II}}(q), \quad U_{\text{III}} = \hbar \frac{R}{L} F_{\text{III}}(q), \quad U_{\text{IV}} = \frac{\hbar}{RC_0} F_{\text{IV}}(r, a), \quad (\text{S10})$$

the resulting forces between the plates are

$$f_{\text{I,IV}} = -\frac{\hbar}{R\varepsilon A} \frac{\partial F_{\text{I,IV}}}{\partial r}, \quad f_{\text{II,III}} = -\frac{\hbar}{R\varepsilon A} \frac{\partial F_{\text{II,III}}}{\partial q}. \quad (\text{S11})$$

For the cases (I)-(III), where we have an analytical expression for  $F$ , the force can be found analytically by simple differentiation. The analytical results are verified by differentiating  $F$  in its integral form and performing the resulting integral numerically. The latter numerical approach is also used for circuit (IV). For all numerical examples plotted in Fig. 3, it was verified that the corresponding validity conditions hold.

## 1.2 Divergence of the potential implies divergence of the force

In the calculation of the van der Waals (vdW) or Casimir forces, it is often the case that ultraviolet divergence encountered in the potential can be avoided by calculating directly the force, namely, by differentiating with respect to the coordinate  $\xi$ . This is since the diverging part does not depend on the coordinate  $\xi$ . For example, in the Casimir or vdW interactions,  $\xi$  is the distance between the interacting objects, whereas the divergence can be thought of as arising from the individual self-interaction of each objects with the vacuum, which does not depend on  $\xi$  [S1, S2].

In contrast, for the zero-point forces inside capacitors considered here, the same ultraviolet divergence of the potential also appears in the force. Intuitively, this is since the frequency-independent capacitance  $C$  does not determine the divergence of the potential. Therefore, a differential of this potential obtained by varying  $C$  should diverge in the same way. In turn, the same is true for a differential, or derivative, with respect to  $\xi$ , via the relation to  $C(\xi)$ . This can be directly shown as follows. The force on  $\xi$  is  $f = -\partial U/\partial \xi = -(\partial U/\partial C)(\partial C/\partial \xi)$ . Since  $\partial C/\partial \xi$

should be finite, the convergence properties of the force are determined by  $\partial U/\partial C$ , obtained from Eq. (3) in the main text as

$$\frac{\partial U}{\partial C} = \int_{-\infty}^{\infty} \frac{d\omega}{2\pi} \hbar \omega \frac{R(\omega)}{[1 + X(\omega)C\omega]^2 + [R(\omega)C\omega]^2} K(\omega), \quad (\text{S12})$$

with

$$K(\omega) = \frac{1 - [X(\omega)C\omega]^2 - [R(\omega)C\omega]^2}{[1 + X(\omega)C\omega]^2 + [R(\omega)C\omega]^2}. \quad (\text{S13})$$

The integrand of Eq. (S12), excluding the function  $K(\omega)$ , is identical to that of the potential, Eq. (3) (up to a frequency-independent factor of  $C$ ). Therefore, if we ignore  $K(\omega)$ , the force should exhibit the same convergence properties as the potential. Focusing now on  $K(\omega)$ , Eq. (S13), consider its effect on the convergence properties of the integrand at high frequencies. Depending on the functions  $X(\omega)$  and  $R(\omega)$ , either one of the three terms 1,  $X(\omega)C\omega$  or  $R(\omega)C\omega$  is the dominant one for  $\omega \rightarrow \infty$ . If it is 1, then  $K(\omega \rightarrow \infty) \rightarrow 1$  and if these are any of the other two, we have  $K(\omega \rightarrow \infty) \rightarrow -1$ . In either case, the function  $K(\omega)$  does not affect the ultraviolet convergence properties of the integral in (S12). Therefore, its convergence properties, and hence those of the force, exactly follow those of the potential.

### 1.3 Possible detection of the forces from Fig. 3

Consider a mechanical oscillator such as the drumhead mode of the capacitor plate from Ref. [S3]. The zero-point electronic force  $f(Z)$  acting on the plate depends on a parameter of the circuit, generally denoted by  $Z$ . For a given circuit with a constant  $Z$ , the resulting static force will shift the plate by

$$x_{dc}(Z) = \frac{f(Z)}{m\Omega^2}, \quad (\text{S14})$$

where  $\Omega$  is the mechanical resonant frequency of the plate and  $m$  its mass. Therefore, in principle, one can infer the function  $f(Z)$  by measuring the plate position  $x$  as a function of  $Z$ , provided that the "signal" value  $x_{dc}(Z)$  is larger than the standard deviation of the noise on  $x$ . This is the essence of the static method. In the dynamic method [S4], we further consider a weak modulation of the circuit parameter around its value  $Z$  in which we wish to measure,  $\delta Z(t) = u \cos(\omega_p t)$ , with  $\omega_p$  is the modulation frequency. Since the modulation is weak,  $u \ll Z$ , we can expand the force as  $f[Z + \delta Z(t)] \approx f(Z) + \delta Z(t) \left. \frac{\partial f}{\partial Z} \right|_Z$  and the equation of motion for the plate position becomes,

$$\ddot{x} + \Gamma \dot{x} + \Omega^2 x = f(Z) + \left. \frac{\partial f}{\partial Z} \right|_Z u \cos(\omega_p t), \quad (\text{S15})$$

where  $\Gamma$  is the mechanical damping of the plate. Solving this in frequency space we obtain the spectrum of the displacement signal (for  $|\omega| > 0$  and in units of  $\text{m}^2\text{Hz}^{-1}$ ),

$$S_x(\omega) = \frac{1}{T_e} |x(\omega)|^2 = \frac{\pi^2}{2m^2} \left[ u \left. \frac{\partial f}{\partial Z} \right|_Z \right]^2 \frac{1}{(\Omega^2 - \omega_p^2)^2 + \omega_p^2 \Gamma^2} [\delta(\omega - \omega_p) + \delta(\omega + \omega_p)], \quad (\text{S16})$$

with  $T_e \rightarrow \int_{-\infty}^{\infty} dt$  being the duration of the experiment. The displacement signal  $x_s(Z)$  (in units of meters) is then obtained by integrating this spectrum with  $\int d\omega/(2\pi)$  over the bandwidth of the modulation and taking the square root. For a modulation bandwidth  $B \ll \Gamma$  around the mechanical resonance  $\Omega$ , this yields

$$x_s(Z) = \frac{\sqrt{\pi}}{m\Gamma\Omega} u \left. \frac{\partial f}{\partial Z} \right|_Z. \quad (\text{S17})$$

Namely, the signal at  $Z$  is proportional to the derivative of force with respect to  $Z$ , evaluated at  $Z$ . In terms of the signal of the static method from Eq.(S14), we find

$$x_s(Z) = \sqrt{\pi} Q \eta(Z) x_{dc}(Z), \quad (\text{S18})$$

where  $Q = \Omega/\Gamma$  is the quality factor of the mechanical resonance and  $\eta(Z) = u \left. \frac{\partial f}{\partial Z} \right|_Z \ll 1$  is a small parameter determined by the adjustable modulation strength  $u$ . In order to be able to measure the force, this signal has to be



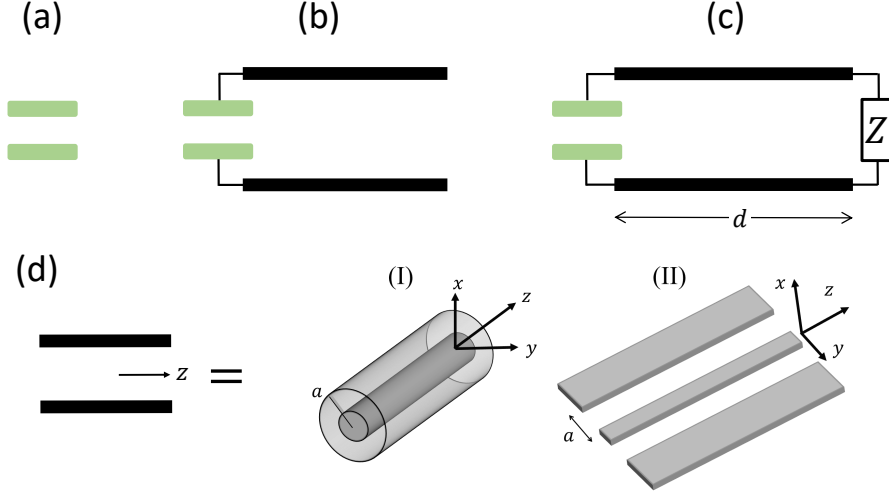


FIG. S1: Casimir forces induced by the electromagnetic vacuum in a transmission-line (TL) circuit (see Sec. 1.4). (a) Two conducting plates (capacitor) in free space exhibit attractive Casimir forces. (b) The same plates connected to a semi-infinite TL exhibit a modified Casimir force. (c) The situation considered in this work is that of a capacitor inside a circuit. Physically, this amounts to two plates (capacitor) coupled to a scatterer with impedance  $Z$ , via the electromagnetic modes of the TL structure. The resulting vacuum-induced (Casimir) force between the plates can be divided to three contributions as per Eq. (S19), including the accounted for by the circuit theory we use (that mediated by the TEM mode). (d) Two examples of TLs. (I) A coaxial line is a “closed” TL in the sense that only guided modes mediated the interaction/force. (II) A coplanar waveguide, extensively used in circuit QED systems [S10, S11], supports mediating non-guided modes as well. The separation between the conductors of the TL is denoted  $a$ .

much larger than the noise in  $x$  contained in the bandwidth  $B$ . Hence the dynamic method may be advantageous for small modulation bandwidth and high  $Q$  of the mechanical resonator.

In order to estimate the possibility to measure the fN scale forces we find in Fig. 3, we consider the physical parameters of the electromechanical capacitor from Ref. [S3]. Beginning with the static method, the signal from Eq. (S14), for a force  $f \sim 1$  fN and mechanical parameters  $m = 48$  pg and  $\Omega = 2\pi \times 10.56$  MHz [S3], is  $x_{dc} \approx 4.7 \times 10^{-18}$  m, which is much smaller than the mechanical zero-point motion of the plate,  $x_{zp} = 4.1 \times 10^{-15}$  m, making the static method irrelevant. Turning to the dynamical method, the displacement sensitivity (noise spectrum) of the device in Ref. [S3], which depends on the magnitude of a probe signal used in the measurement, reaches an optimum of  $5.5 \times 10^{-34} \text{ m}^2 \text{ Hz}^{-1}$ . Considering non-optimal operation, we take  $S_N(\omega) \sim 10^{-32} \text{ m}^2 \text{ Hz}^{-1}$  over the bandwidth of interest. The noise signal,  $x_N = \sqrt{S_N B}$ , for  $Q = 3.3 \times 10^5$  [S3] and a bandwidth of e.g.  $B = 0.01\Gamma = 0.01\Omega/Q$ , is  $x_N = 1.4 \times 10^{-16}$  m. Comparing it to the signal, Eq. (S17), with a modulation strength of e.g.  $\eta = 0.05$ , we find  $x_s \approx 1.4 \times 10^{-13}$  m, three orders of magnitude larger than the noise. Such a signal-to-noise ratio is likely to be sufficient in order to resolve forces such as those from Fig. 3.

#### 1.4 Distinction between electronic zero-point forces and Casimir forces induced by the electromagnetic vacuum

An important aspect of the possibility to measure the electronic zero-point forces as a function of circuit parameters is the ability to distinguish them from other forces that act between the capacitor plates. Such an ability naturally relies on the assumption that these other forces do not change with the circuit parameters  $Z$ , therefore yielding only a constant shift to the force as a function of  $Z$ . In the following we examine this assumption for dipolar-like forces, using the example of the Casimir force induced by the electromagnetic vacuum in a circuit environment.

A pair of parallel plates (the capacitor) in free space will exhibit an attractive force due to their interaction with the vacuum fluctuations of the plane-wave electromagnetic modes of free space, the well-known Casimir force (Fig. S1a). Consider now that the two capacitor plates are embedded in an infinite transmission line (TL), namely, they are connected to infinitely-long circuit wires (Fig. S1b). The electromagnetic modes supported by the TL are different than those of free space, and correspondingly may lead to a slightly modified vacuum-induced Casimir force, denoted

$f_C^{(0)}$ . The case that we are concerned with however is that of Fig. 1Sc, where the capacitor is embedded in a TL of length  $d$ , terminated by a general impedance  $Z$ . The force between the plates in this case can be written as

$$f_C(Z, d) = f_C^{(0)} + \delta f_C(Z, d), \quad \delta f_C(Z, d) = \delta f_{\text{TEM}}(Z, d) + \delta f_{\text{other}}(Z, d). \quad (\text{S19})$$

Here  $f_C^{(0)}$  is the component of the force just due the fact that the capacitor is embedded inside a TL (as in Fig. S1b), whereas  $\delta f_C(Z, d)$  is the component due to the *interaction* between the capacitor and the scatterer  $Z$ , mediated by the electromagnetic modes of the TL structure. The latter component is in turn divided into its contribution mediated by the TEM mode and that mediated by all other transverse modes supported by the structure. The TEM mode is the fundamental transverse mode of a TL. It has a frequency-independent transverse profile, characterized by a constant line impedance (equivalently, by an effective area), and a linear dispersion relation, so that it forms the 1d propagating plane waves that are taken into account by circuit theory (possibly, including the lumped-circuit assumption,  $c/d \ll \omega$ , for all relevant  $\omega$ 's, see below). The rest of the modes ("other") consist of an infinite series of guided modes which possess a cutoff frequency larger than  $c/a$  ( $a$  being the conductors that form the TL, see Fig. S1d), and whose transverse profile and dispersion depend on the structure of the TL, such as the TE and TM modes of a coaxial line [Fig. S1d(I)] [S5]. For an open planar transmission line, such as the coplanar waveguide [Fig. S1d(II)] or a microstrip, there are additional non-guided modes.

Let us now examine the role of each of the contributions to the force. The force that we calculated using our circuit theory is  $\delta f_{\text{TEM}}(Z, d)$ . The length  $d$  does not appear in our calculation since it can be absorbed in the impedance  $Z$  by using the reflection properties of impedances in TL theory [S6], or by simply assuming that the circuit is lumped,  $\omega \ll c/d$  for any relevant  $\omega$  (namely,  $\omega$  values below the effective cutoff of the converging integrals we calculate). The contribution due to the introduction of the vacuum of the TL modes,  $f_C^{(0)}$ , does not depend on  $Z$ , and hence only gives a constant shift to the measurement as a function of  $Z$ . The *main question* is then, whether the component  $\delta f_{\text{other}}(Z, d)$ , which is *not* taken into account by our circuit theory and which *does* depend on  $Z$ , gives a contribution large enough to mask the "signal"  $\delta f_{\text{TEM}}(Z, d)$ .

In order to answer this question, consider first the contribution to  $\delta f_{\text{other}}(Z, d)$  which is mediated by the guided modes with a cutoff frequency. In Refs. [S7, S8], it is shown that the vdW potential mediated by these modes between two scatterers (the capacitor and  $Z$  in our case) is suppressed exponentially with the distance  $d$  scaled to the width  $a$ , so that for  $d \gg a$ , they are negligible with respect to the TEM circuit-theory contribution. For TLs used in circuit QED experiments,  $a \sim 1\mu\text{m}$ , which is much smaller than the relevant wavelengths  $\lambda = 2\pi c/\omega$ , so that it should be natural to work in the regime  $\lambda \gg d \gg a$ , where  $\delta f_{\text{other}}(Z, d)$ , mediated by guided modes, is negligible and can be ignored. In a coaxial TL, these are the only "other" modes that exist apart from the TL, so that our theory can be readily applied there. For an open TL, such as the coplanar waveguide (Fig. S2b), we should also consider the contribution to  $\delta f_{\text{other}}(Z, d)$  from non-guided modes. These modes resemble free-space modes and therefore are expected to give an interaction  $\delta f_{\text{other}}(Z, d)$  that decays as a power-law with distance, e.g.  $1/d^7$  for weak scatterers (force resulting from vdW interaction). Again, by choosing sufficiently long  $d$ , these forces can become negligible with respect to those mediated by the TEM modes (captured by our circuit theory), which e.g. in the vdW case decay much slower, as  $1/d^4$  [S7].

To conclude, we have considered the electromagnetic zero-point forces between polarized objects, which are not accounted for in our circuit theory. We have generally shown that by properly choosing the distance  $d$ , the dependence of these forces on  $Z$  [namely, the component  $\delta f_{\text{other}}(Z, d)$ ] can be effectively eliminated. The specific required length of  $d$  depends on the TL system we consider, and can range from a few microns ( $d \gg a$ ) in a closed TL to e.g. a few microwave wavelengths ( $d \gg \lambda$ ) in the planar open TL case (recall that in such a case the lumped circuit description is valid when  $Z$  absorbs the length  $d$  using impedance reflection properties of TL theory).

## 2. CALCULATION OF LEVEL SHIFTS INDUCED IN A SUPERCONDUCTING TRANSMON QUBIT

### 2.1 Weak coupling: dissipative circuit as a reservoir

Consider the circuit from Fig. 1d in the main text. It can be divided into two systems; namely, the circuit  $Z$  and the superconducting qubit (SCQ). Out of the many degrees of freedom that these systems may possess, and following the Hamiltonian description of circuits [S9], we focus on the two degrees of freedom that appear in Fig. 1d, that is, the circuit nodes  $a$  and  $J$ , belonging to the systems  $Z$  and  $J$ , respectively ( $J$  denoting the SCQ). Each circuit node is represented by a dynamical variable (operator), e.g. voltage  $\hat{V}_m(t)$  ( $m = a, J$ ), or more commonly the "flux" defined by  $\hat{\phi}_m(t) = \int_0^t dt' \hat{V}_m(t')$ . Then, the interaction between the systems  $Z$  and  $J$ , coupled by the capacitor  $C_g$ , is given

by [S9–S11]

$$H_{ZJ} = \frac{C_g}{C_g + C_J} \hat{V}_a \hat{Q}_J, \quad (\text{S20})$$

where  $\hat{Q}_J$  is the canonical conjugate of  $\hat{\phi}_J$  and  $C_J$  is the total capacitance of the SCQ (for a transmon qubit this capacitance includes that related to the Josephson junctions and an additional large capacitance [S11]). For weak coupling  $C_g \ll C_J$ , we can take the rest of the Hamiltonian as that of the two noninteracting systems. For the SCQ this Hamiltonian is [S9–S11]

$$H_J = \frac{\hat{Q}_J^2}{2C_J} - E_J \cos\left(\frac{2e}{\hbar} \hat{\phi}_J\right) = \sum_n E_n |n\rangle \langle n|, \quad (\text{S21})$$

with  $e$  the electron charge and  $E_J$  the Josephson energy, and where  $|n\rangle$  are the eigenstates of  $H_J$  with eigenenergies  $E_n$ . The system  $Z$  is assumed to be a linear circuit which may include resistive elements (dissipation). In the Hamiltonian formalism, such a dissipative system can be described by the Hamiltonian  $H_Z$  of a continuous spectrum of Harmonic oscillators. However, in order to describe the effect of this dissipative system on the SCQ, we would not need to use such a detailed model. Instead, we will treat the dissipative system as a *reservoir* to which the SCQ system is damped. This will allow us to use the tools of quantum open systems which do not depend on the structure of  $H_Z$ , rather only on the noninteracting statistics of  $\hat{V}_a$ .

## 2.2 Effective Hamiltonian induced by the reservoir

Moving to an interaction picture with respect to the noninteracting part of the Hamiltonian,  $H_J + H_Z$ , the Hamiltonian becomes,

$$H_I(t) = \beta \tilde{V}_a(t) \tilde{Q}_J(t), \quad (\text{S22})$$

with the tilded operators in the interaction picture, and with  $\beta = C_g(C_g + C_J) \approx C_g/C_J \ll 1$ . Assuming the weak-coupling regime between the system and the reservoir, we can derive a quantum master equation for the SCQ system damped by the reservoir  $Z$ . This can be done as usual by assuming a stationary state for the reservoir and using the Fourier expansion  $\tilde{V}_a(t) = \int d\omega/(2\pi) V_a(\omega) e^{-i\omega t}$ , where  $V_a(\omega)$  and  $V_a(-\omega) = \hat{V}_a^\dagger(\omega)$  take the role of the harmonic oscillator lowering and rising operators of the reservoir, in more standard derivations [S12, S13]. The result is a Markovian master equation from which we can deduce the effective non-hermitian correction to the SCQ Hamiltonian, induced by the reservoir,

$$H_{\text{eff}} = \sum_{n,m} E_{nm}^{(2)} |n\rangle \langle m|, \quad E_{nm}^{(2)} = \frac{\beta^2}{\hbar} \sum_{n'} Q_{nn'} Q_{n'm} \left[ -\Delta(\omega_{nn'}) - \frac{i}{2} S_{V_a}(\omega_{nn'}) \right]. \quad (\text{S23})$$

Here the pairs of states  $n, m$  are either identical or degenerate,  $Q_{nn'} = \langle n | \hat{Q}_J | n' \rangle$ ,  $\omega_{nn'} = (E_n - E_{n'})/\hbar$ , and

$$S_{V_a}(\omega) = \int_{-\infty}^{\infty} dt e^{i\omega t} \langle \tilde{V}_a(t) \tilde{V}_a(0) \rangle = \frac{1}{T_e} \langle V_a(\omega) V_a(-\omega) \rangle, \quad \Delta(\omega) = \frac{1}{2\pi} \text{P} \int_{-\infty}^{\infty} d\omega' \frac{S_{V_a}(\omega')}{\omega' - \omega}. \quad (\text{S24})$$

This is a general Markovian result for a system with a discrete spectrum  $\{|n\rangle\}$  coupled to a reservoir noise  $\beta V_a(t)$  via a system operator  $Q_J$ . As usual, the only information we need about the reservoir is the noise spectrum  $S_{V_a}(\omega)$  in the absence of interaction with the system (i.e., in the interaction picture). In our case, we can simply calculate it from Kirchhoff's laws, by finding the voltage  $V_a(\omega)$  induced by the quantum noise sources in the given circuit  $Z$ .

## 2.3 Shift in a transmon qubit coupled to an RC circuit

Consider now the specific case of a transmon SCQ, in the regime  $E_J \gg E_C = e^2/(2C_J)$ , where the nonlinearity of the SCQ is weak. The matrix elements  $Q_{nn'}$  are then approximated by those of a harmonic oscillator, whereas the weak nonlinearity appears in the eigenenergies of the states  $n = 0, 1, 2, \dots$  [S11],

$$|Q_{nn'}| \approx 2e \left( \frac{E_J}{8E_C} \right)^{\frac{1}{4}} \left[ \delta_{n',n+1} \sqrt{\frac{n+1}{2}} + \delta_{n',n-1} \sqrt{\frac{n}{2}} \right], \quad E_{n+1} - E_n = \hbar\omega_0 - E_C(n+1), \quad \hbar\omega_0 = \sqrt{8E_C E_J}. \quad (\text{S25})$$

Noting also that these eigenstates are non-degenerate, the effective Hamiltonian can only give rise an energy shift and width of each state, induced by the reservoir. Considering the first two states,  $n = 0, 1$ , we use (S25) inside (S23) and obtain the general expressions for the energy shift of the transition,  $\delta = \text{Re}\{E_1^{(2)} - E_0^{(2)}\}$ , and the correction to its width,  $\gamma = \text{Im}\{E_1^{(2)}\}$ , Eq. (5) of the main text.

Considering the specific case of the  $RC$  circuit in the bottom of Fig. 1d, we easily find  $V_a(\omega) = I_N(\omega)R/(1-i\omega CR)$ , so that  $S_{V_a}(\omega) = 2\hbar\omega R/(1+\omega^2 C^2 R^2)$  (for  $\omega > 0$ ). Inserting this into the expressions for  $\delta$  and  $\gamma$  in the main text and performing the integrations in  $\delta$ , we then obtain

$$\begin{aligned}\delta &= \frac{\beta^2}{\pi} \frac{R}{Z_J} \omega_0 [I_1 - I_2], \quad I_1 = -\frac{(-1+x_c)\ln(b-bx_c)}{1+b^2(-1+x_c)^2}, \quad I_2 = \frac{\pi + b(2-4x_c)\ln(b-2bx_c)}{2[b+b^3(1-2x_c)^2]}, \\ \gamma &= \beta^2 \frac{R}{Z_J} \omega_0 \frac{1-x_c}{1+b^2(1-x_c)^2}, \quad x_c = \frac{E_C}{\hbar\omega} = \sqrt{\frac{E_C}{8E_J}}, \quad b = \omega_0 CR,\end{aligned}\tag{S26}$$

with  $Z_J = (\hbar/e^2)\sqrt{E_C/2E_J}$ . We note that for a transmon we have  $x_c \ll 1$ , and if we further assume  $b \ll 1$ , we obtain  $I_1 - I_2 \approx -\pi/(2b)$  and  $\gamma \approx \beta^2 \omega_0 R/Z_J$  as in the main text.

- 
- [S1] E. Shahmoon, in *Forces of the Quantum Vacuum* (W. M .R. Simpson and U. Leonhardt, Eds.), Ch. 3 (World Scientific, 2015).
  - [S2] P. W. Milonni, *The Quantum Vacuum: An Introduction to Quantum Electrodynamics* (Academic, 1993).
  - [S3] J. D. Teufel, T. Donner, Dale Li, J. W. Harlow, M. S. Allman, K. Cicak, A. J. Sirois, J. D. Whittaker, K. W. Lehnert and R. W. Simmonds, *Nature* **475**, 359 (2011).
  - [S4] R. S. Decca, in *Forces of the Quantum Vacuum* (W. M .R. Simpson and U. Leonhardt, Eds.), Ch. 5 (World Scientific, 2015).
  - [S5] J. P. Donohoe, *Microwave Theory* (online lecture notes. <http://www.ece.msstate.edu/~donohoe/ece4333.html>).
  - [S6] Pozar DM (2005) *Microwave Engineering* (John Wiley and Sons).
  - [S7] E. Shahmoon, I. Mazets and G. Kurizki, *Proc. Natl. Acad. Sci.* **111**, 10485 (2014).
  - [S8] E. Shahmoon E and G. Kurizki *Phys. Rev. A* **87**, 062105 (2013).
  - [S9] M. H. Devoret, *Quantum Fluctuations in Electrical Circuits*, in *Quantum Fluctuations*, Les Houches Session LXIII, pp. 351 (Elsevier 1997).
  - [S10] A. Blais, R. S. Huang, A. Wallraff, S. M. Girvin and R. J. Schoelkopf, *hys. Rev. A* **69**, 062320 (2004).
  - [S11] J. Koch, T. M. Yu, J. Gambetta, A. A. Houck, D. I. Schuster, J. Majer, A. Blais, M. H. Devoret, S. M. Girvin, and R. J. Schoelkopf, *Phys. Rev. A* **76**, 042319 (2007).
  - [S12] H. J. Carmichael, *Statistical Methods in Quantum Optics 1* (Springer, 1998).
  - [S13] E. Shahmoon and G. Kurizki, *Phys. Rev. A* **89**, 043419 (2014).